Cell, Vol. 80, 795–803, March 10, 1995, Copyright © 1995 by Cell Press

A Molecular Basis for Cardiac Arrhythmia: *HERG* Mutations Cause Long QT Syndrome

Mark E. Curran,*† Igor Splawski,*† Katherine W. Timothy,‡ G. Michael Vincent,‡§ Eric D. Green,# and Mark T. Keating*†‡‖
*Department of Human Genetics
†Eccles Program in Human Molecular Biology and Genetics
‡Cardiology Division
‖Howard Hughes Medical Institute
University of Utah Health Sciences Center
Salt Lake City, Utah 84112
§Department of Medicine
Latter Day Saints Hospital
Salt Lake City, Utah 84037
#National Center for Human Genome Research
National Institutes of Health
Bethesda, Maryland 20892

Summary

To identify genes involved in cardiac arrhythmia, we investigated patients with long QT syndrome (LQT), an inherited disorder causing sudden death from a ventricular tachyarrhythmia, torsade de pointes. We previously mapped LQT loci on chromosomes 11 (*LQT1*), 7 (*LQT2*), and 3 (*LQT3*). Here, linkage and physical mapping place *LQT2* and a putative potassium channel gene, *HERG*, on chromosome 7q35-36. Single strand conformation polymorphism and DNA sequence analyses reveal *HERG* mutations in six LQT families, including two intragenic deletions, one splice-donor mutation, and three missense mutations. In one kindred, the mutation arose de novo. Northern blot analyses show that *HERG* is strongly expressed in the heart. These data indicate that *HERG* is *LQT2* and suggest a likely cellular mechanism for torsade de pointes.

Introduction

Long QT syndrome (LQT) is an inherited cardiac disorder that causes syncope, seizures, and sudden death, usually in young, otherwise healthy individuals (Ward, 1964; Romano, 1965; Schwartz et al., 1975). Most LQT gene carriers manifest prolongation of the QT interval on electrocardiograms, a sign of abnormal cardiac repolarization (Vincent et al., 1992). The clinical features of LQT result from episodic cardiac arrhythmias, specifically torsade de pointes, named for the characteristic undulating nature of the electrocardiogram in this arrhythmia. Torsade de pointes may degenerate into ventricular fibrillation, a particularly lethal arrhythmia. Although LQT is not a common diagnosis, ventricular arrhythmias are very common; more than 300,000 Americans die suddenly every year (Kannel et al., 1987; Willich et al., 1987), and in many cases the underlying mechanism may be aberrant cardiac repolarization. LQT, therefore, provides a unique opportunity to study life-threatening cardiac arrhythmias at the molecular level.

A molecular basis for LQT was not previously known. In 1991, we discovered tight linkage between autosomal dominant LQT and a polymorphism at H-*RAS* (Keating et al., 1991a). This discovery localized an LQT gene (*LQT1*) to chromosome 11p15.5 and made genetic testing possible in some families. Autosomal dominant LQT was previously thought to be genetically homogeneous, and the first seven families that we studied were linked to 11p15.5 (Keating et al., 1991b). In 1993, however, several laboratories, including our group, identified families that were not linked to chromosome 11p15.5 (Benhorin et al., 1993; Curran et al., 1993a; Towbin et al., 1994). In 1994, we identified two additional LQT loci, *LQT2* on chromosome 7q35-36 (nine families) and *LQT3* on chromosome 3p21-24 (three families) (Jiang et al., 1994). Since three families in our study remained unlinked, at least one more LQT locus exists. This degree of heterogeneity suggests that distinct LQT genes may encode proteins that interact to modulate cardiac repolarization and arrhythmia risk.

Since LQT is associated with abnormal cardiac repolarization, genes that encode ion channels (or their modulators) are reasonable candidates. H-*RAS*, which was localized to chromosome 11p15.5, was excluded as a candidate for *LQT1* based on direct DNA sequence analyses (unpublished data) and by linkage analyses (Roy et al., 1994). A skeletal muscle chloride channel (*CLCN1*; Koch et al., 1992) and a cardiac muscarinic–acetylcholine receptor (*CHRM2*; Bonner et al., 1987) became candidates for *LQT2* based on their chromosome 7q35-36 location, but subsequent linkage analyses have excluded these genes (Wang et al., submitted).

Warmke and Ganetzky (1994) identified a novel human cDNA, the human *ether-a-go-go*-related gene (*HERG*). *HERG* was localized to human chromosome 7 by polymerase chain reaction (PCR) analysis of a somatic cell hybrid panel (Warmke and Ganetzky, 1994). The function of the protein encoded by *HERG* is not known, but it has predicted amino acid sequence homology to potassium channels. *HERG* was isolated from a hippocampal cDNA library by homology to the Drosophila *ether-a-go-go* (*eag*) gene, which encodes a Ca^{2+}-modulated potassium channel (Bruggeman et al., 1993). *HERG* is not the human homolog of *eag*, however, their products sharing only ~50% amino acid sequence homology.

In this study, we provide evidence indicating that *HERG* is *LQT2*. First, we identified and characterized new LQT families and showed that all were linked to markers on chromosome 7q35-36, confirming the location of *LQT2*. Second, we mapped *HERG* to chromosome 7q35-36, making *HERG* a candidate gene for *LQT2*. Third, we demonstrated that *HERG* is strongly expressed in the heart. Finally, we identified six *HERG* mutations associated with LQT; one of these mutations arose de novo.

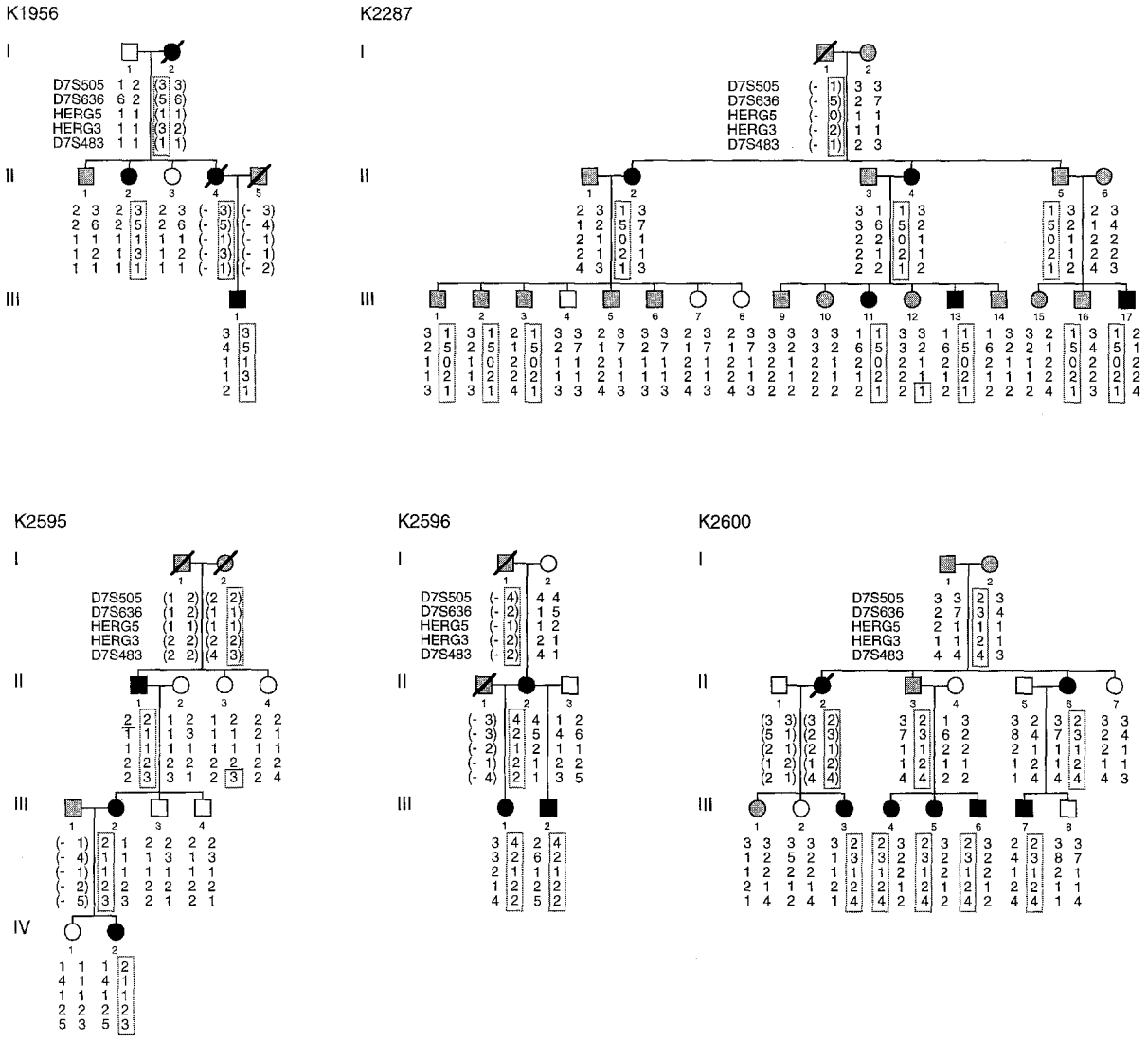

Figure 1. Pedigree Structure and Genotypic Analyses of Five LQT Families

Individuals showing the characteristic features of LQT, including prolongation of the QT interval and history of syncope, seizures, or aborted sudden death, are indicated by closed circles (females) or closed squares (males). Unaffected individuals are indicated by open circles or open squares. Individuals with an equivocal phenotype or those for whom phenotypic data are unavailable are shown as stippled. Circles or squares with a slash denote deceased individuals. Haplotypes for polymorphic markers linked to *LQT2* are shown under each individual. These markers include (centromere to telomere) *D7S505*, *D7S636*, *HERG 5-11*, *HERG 3-8*, and *D7S483* (Gyapay et al., 1994; Wang et al., submitted). Haplotypes cosegregating with the disease phenotype are indicated by a box. Recombination events are indicated with a horizontal black line. Informed consent was obtained from all individuals or from their guardians in accordance with local institutional review board guidelines. Haplotype analyses indicate that the LQT phenotype in these kindreds is linked to markers on chromosome 7q35-36.

Results

LQT2 Is Linked to Markers on Chromosome 7q35-36

To determine the relative frequency of the three known LQT loci (*LQT1*, *LQT2*, and *LQT3*), we performed linkage analyses in families with this disorder. Five LQT families were identified and phenotypically characterized (Figure 1). These families were unrelated and of varying descent, including Mexican (Spanish), German, English, and Danish. In each case, an autosomal dominant pattern of inheritance was suggested by inspection of the pedigree. Affected individuals were identified by the presence of QT prolongation on electrocardiograms and, in some cases, a history of syncope or aborted sudden death. No patients had signs of congenital neural hearing loss, a finding associated with the rare autosomal recessive form of LQT, or other phenotypic abnormalities. Genotype analyses with polymorphic markers linked to the known LQT loci suggested that the disease phenotype in these families was linked to polymorphic markers on chromosome 7q35-36 (Figure 1). The maximum combined two-point lod score for these five families was 5.13 at *D7S636* ($\theta = 0.0$; Table 1). When combined with our previous studies (Jiang et al.,

Table 1. Maximum Pairwise Lod Scores, Recombination Fractions for Linkage of *LQT2* with *HERG*, and Polymorphic Markers on Chromosome 7

	Families from Present Study		Families Studied to Date	
Locus	Z_{max}	θ	Z_{max}	θ
D7S505	4.40	0.0	22.91	0.009
D7S636	5.13	0.0	26.14	0.00
HERG 3-8	0.11	0.0	6.34	0.00
HERG 5-11	3.55	0.0	9.64	0.00
D7S483	2.48	0.0	22.42	0.00

Markers are shown in chromosomal order (centromere to telomere) (Gyapay et al., 1994). The first column (families from present study) indicates combined lod scores for the five families described in this study. The second column (families studied to date) indicates combined lod scores from the five families studied here, as well as the nine families from our previous study (Jiang et al., 1994). Z_{max} indicates maximum lod score; θ indicates estimated recombination fraction at Z_{max}.

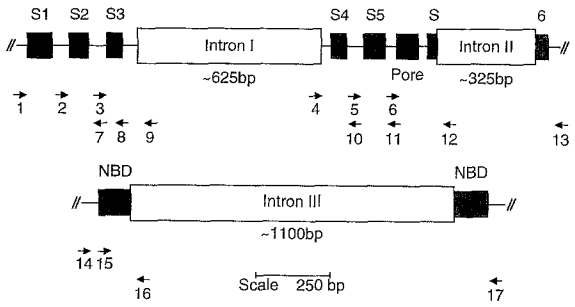

Figure 2. Partial Genomic Structure of *HERG* and Location of PCR Primers Used in This Study

Regions encoding predicted membrane-spanning domains (S1–S6), the pore domain, and the nucleotide-binding domain (NBD) are indicated. The DNA sequences for the intron–exon boundaries are these: intron I, 5′-AGGAGgtgggg...ccccagCTGATC-3′; intron II, 5′-TGGCTgtgagt...ccccagCCCTC-3′; intron III, 5′-CCTGGgtatgg...ctccagGGAAG-3′.

1994; Wang et al., submitted), the maximum combined two-point lod score for the 14 chromosome 7–linked families was 26.14, also at *D7S636* (θ = 0.0; Table 1). Haplotype analyses were consistent with our previous studies, placing *LQT2* between *D7S505* and *D7S483* (Figure 1; Wang et al., submitted), localizing this gene to chromosome 7q35-36.

HERG Maps to Chromosome 7q35-36

HERG was previously mapped to chromosome 7 (Warmke and Ganetzky, 1994). To test the candidacy of this gene, we refined the localization of *HERG* using two physical mapping techniques. First, we mapped *HERG* on a set of yeast artificial chromosome (YAC) contigs constructed for chromosome 7 (Green et al., 1994). *HERG* was localized to the same YAC as *D7S505*, a polymorphic marker that was tightly linked to *LQT2* (Table 1). Second, we mapped *HERG* to chromosome 7q35-36 using fluorescent in situ hybridization (FISH) with a P1 genomic clone containing *HERG* (data not shown).

To determine whether *HERG* was genetically linked to the LQT locus, we used single strand conformation polymorphism (SSCP) analyses to identify polymorphisms within *HERG* and performed linkage analyses in the chromosome 7–linked families. Two aberrant SSCP conformers were identified in DNA samples from patients and controls using primer pairs *5-11* and *3-8* (Figure 2). These conformers were cloned and sequenced. One abnormal conformer resulted from a C to T substitution at position 3 of codon 489 (cDNA nucleotide 1467; observed heterozygosity of 0.37). The second abnormal conformer resulted from an A to G substitution at position 3 of codon 564 (cDNA nucleotide 1692; observed heterozygosity of 0.44). Neither substitution affected the predicted amino acid sequence of HERG. *HERG* polymorphisms were used for genotypic analyses in chromosome 7–linked families (see Figure 1; data not shown). No recombination events between *HERG* and LQT were identified in any of these families. The maximum combined lod score for the 14 families was 9.64 (θ = 0.0; Table 1). These data indicate that *HERG* is completely linked to *LQT2*.

HERG Intragenic Deletions Associated with LQT in Two Families

To test the hypothesis that *HERG* is *LQT2*, we used SSCP analyses to screen for mutations in affected individuals. Since the genomic structure of *HERG* was unknown, oligonucleotide primer pairs were designed from published (Warmke and Ganetzky, 1994) *HERG* cDNA sequences (Figure 2; Table 2). In most cases, single products of expected size were generated. For primer pairs *1-10*, *6-13*, and *15-17*, however, products of greater than expected size were obtained, suggesting the presence of intronic sequences. To examine this possibility, we cloned and sequenced these larger products. DNA sequence analyses identified three introns at positions 1557/1558, 1945/

Table 2. *HERG* PCR Primers

Name	Position	Sequence
1 L	1147–1166	GACGTGCTGCCTGAGTACAA
2 L	1291–1312	TTCCTGCTGAAGGAGACGGAAG
3 L	1417–1437	ACCACCTACGTCAATGCCAAC
4 L	Intron I	TGCCCCATCAACGGAATGTGC
5 L	1618–1636	GATCGCTACTCAGAGTACG
6 L	1802–1823	GCCTGGGCGGCCCCTCCATCAA
7 R	1446–1426	CACCTCCTCGTTGGCATTGAC
8 R	1527–1503	GTCGAAGGGGATGGCGGCCACCATG
9 R	Intron I	TACACCACCTGCCTCCTTGCTGA
10 R	1643–1623	GCCGCGCCGTACTCTGAGTAG
11 R	1758–1736	CAGCCAGCCGATGCGTGAGTCCA
12 R	Intron II	GCCCGCCCCTGGGCACACTCA
13 R	2034–2016	CAGCATCTGTGTGTGGTAG
16 R	Intron III	GGCATTTCCAGTCCAGTGC
15 L	2259–2278	CCTGGCCATGAAGTTCAAGA
14 L	2214–2233	GCACTGCAAACCCTTCCGAG
17 R	2550–2529	GTCGGAGAACTCAGGGTACATG

All primers are shown in 5′ to 3′ direction. Sense strand oligonucleotides are indicated with an L and antisense oligonucleotides are indicated with an R. cDNA sequence was obtained from the GenBank data base; nucleotide numbering begins with the initiator methionine.

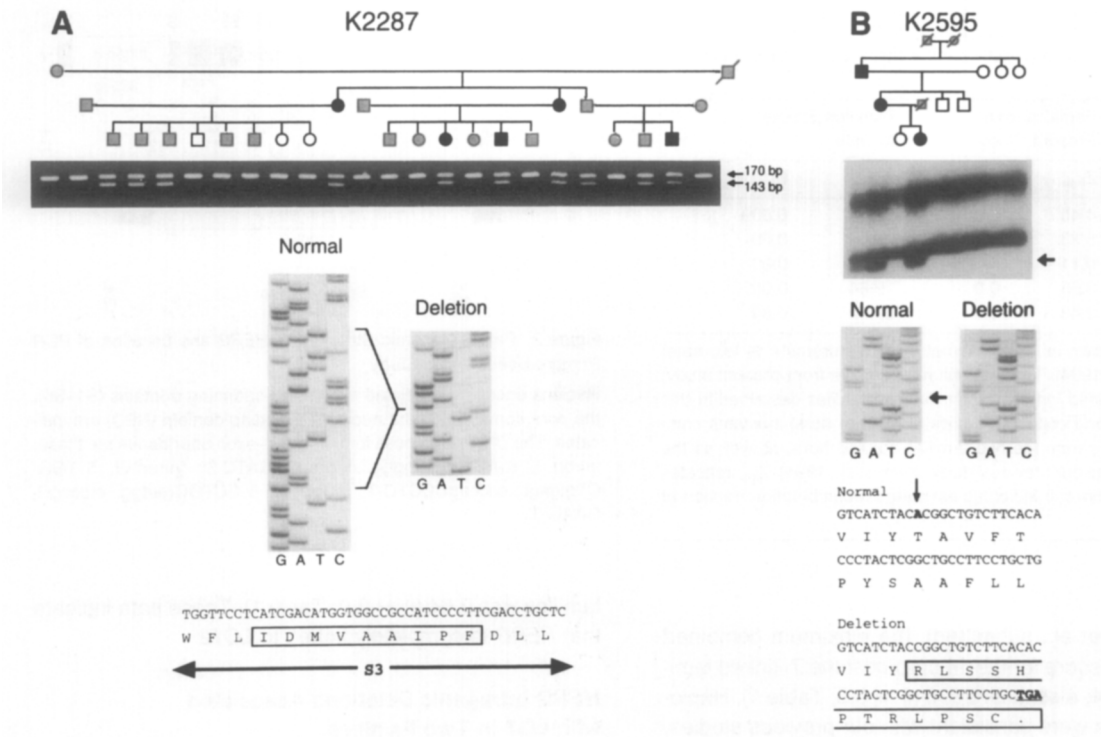

Figure 3. *HERG* Intragenic Deletions Associated with LQT in Two Families

(A) Pedigree structure of K2287, results of PCR amplification using primer pair *3-9*, and the effect of the deletion on the predicted structure of HERG protein are shown. Note that an aberrant fragment of 143 bp is observed in affected members of this kindred, indicating the presence of a disease-associated intragenic deletion. DNA sequence of normal and aberrant PCR products defines a 27 bp deletion (ΔI500-F508). This mutation causes an in-frame deletion of nine amino acids in the third membrane-spanning domain (S3). Deleted sequences are indicated.

(B) Pedigree structure of K2595 is shown. Deceased individuals are indicated by a slash. The results of SSCP analyses using primer pair *1-9* are shown beneath each individual. Note that an aberrant SSCP conformer cosegregates with the disease in this family. DNA sequence shows a single base pair deletion (Δ1261). This deletion results in a frameshift followed by a stop codon 12 amino acids downstream. The deleted nucleotide is indicated with an arrow.

1946, and 2398/2399 of the cDNA sequence (Figure 2). These boundaries were confirmed by direct DNA sequencing of *HERG* genomic clones containing *HERG* (data not shown). To facilitate SSCP analyses, we designed additional primers to intronic sequences.

As indicated previously, SSCP analyses using primer pair *3-8* identified an A to G polymorphism within *HERG* (cDNA nucleotide 1692). Analysis of kindred 2287 (K2287) using this SSCP defined a pattern of genotypes consistent with a null allele (see Figure 1). Possible explanations for these findings included multiple misinheritances, a possibility not supported by our previous genotypic analyses, DNA sample errors, base pair substitutions, or a deletion. To test the hypothesis that the genotypic data were due to a small deletion, we repeated PCR analyses of K2287 using a new primer pair (*3-9*) flanking the previous set of primers. These experiments identified two products of 170 bp and 143 bp in affected members of K2287 (Figure 3A). By contrast, only a single product of 170 bp was observed in unaffected members of this kindred. Furthermore, only the 170 bp band was seen in DNA samples from more than 200 unaffected individuals (data not shown). The 143 bp and 170 bp products were cloned from affected individual II-2. Direct sequence analyses of the aberrant PCR product revealed the presence of a 27 bp deletion beginning at position 1498 (ΔI500-F508). This deletion disrupts the third membrane-spanning domain (S3) of HERG.

To test further the hypothesis that *HERG* is *LQT2*, we continued SSCP analyses in additional kindreds. SSCP using the primer pair *1-9* identified an aberrant conformer in affected individuals of K2595 (Figure 3B). Analyses of more than 200 unaffected individuals failed to show this anomaly (data not shown). The normal and aberrant conformers were cloned and sequenced, revealing a single base deletion at position 1261 (Δ1261). This deletion results in a frameshift in sequences encoding the first membrane-spanning domain (S1), leading to a new stop codon within 12 amino acids. The identification of intragenic deletions of *HERG* in two LQT families suggests that *HERG* mutations can cause LQT.

Three *HERG* Point Mutations Associated with LQT

To identify additional *HERG* mutations in *LQT2*, we continued SSCP analyses in linked kindreds and sporadic cases. Three aberrant SSCP conformers were identified in affected members of K1956, K2596, and K2015 (Figure 4). In each case, the normal and aberrant conformers were cloned and sequenced. In K1956, a C to T substitution at position 1682 was identified. This mutation results in substitution of valine for a highly conserved alanine at

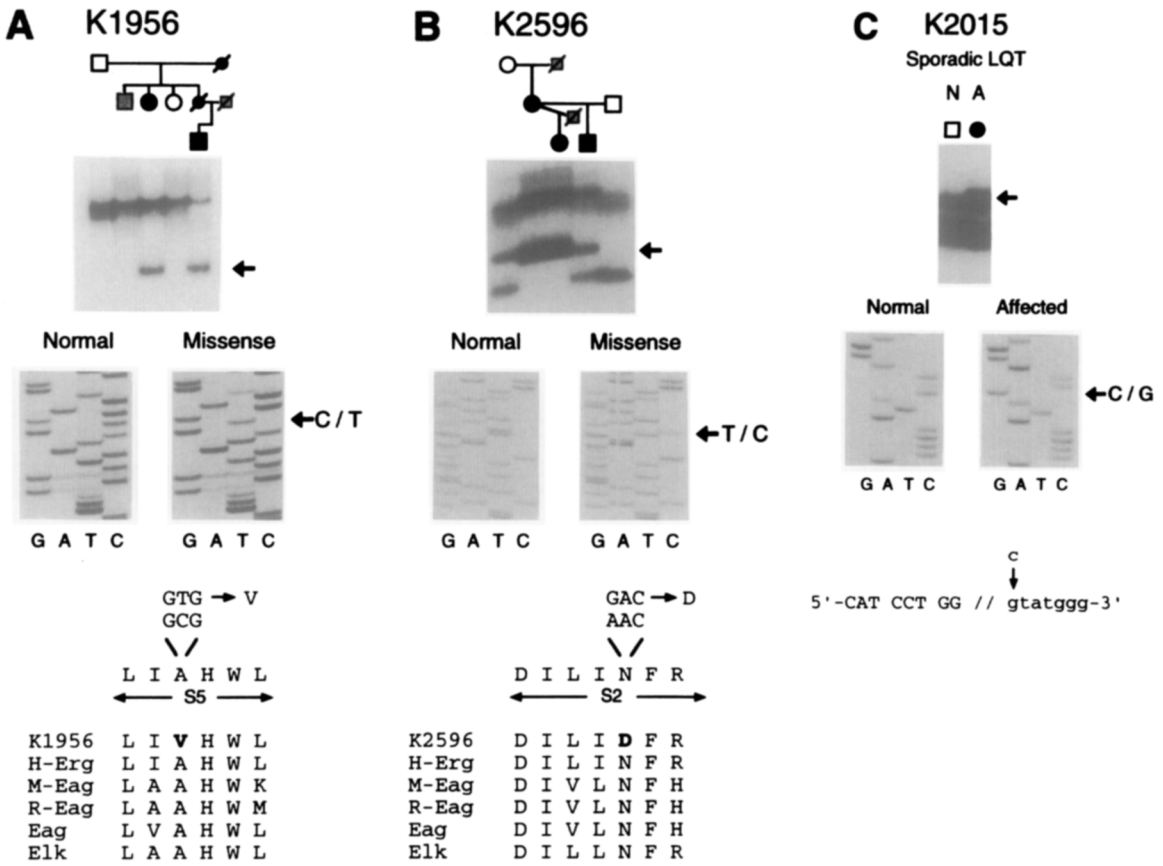

Figure 4. *HERG* Point Mutations Identified in Three LQT Kindreds

Pedigree structure of K1956 (A), K2596 (B), and K2015 (C) are shown. Below each pedigree, the results of SSCP analyses with primer pair *5-11* (K1956), primer pair *1-9* (K2596), and primer pair *14-16* (K2015) are shown. Aberrant SSCP conformers cosegregate with the disease in each kindred. DNA sequence analyses of the normal and aberrant conformers reveals a C to T substitution at position 1682 in K1956. This mutation results in substitution of valine for a highly conserved alanine residue at codon 561 (A561V). Analyses of K2596 reveals an A to G substitution at position 1408 (T to C substitution on the antisense strand is shown). This mutation results in substitution of aspartic acid for a conserved asparagine in the second transmembrane domain (N470D). Analyses of K2015 reveals a G to C substitution (C to G substitution on the antisense strand is shown). This mutation occurs in the splice-donor sequence of intron III. Coding sequences are shown in uppercase and intronic sequences are lowercase. Note that the G to C substitution disrupts the splice-donor site (*HERG*, *M-eag*, *elk* [Warmke and Ganetzky, 1994]; *R-eag* [Ludwig et al., 1994]).

codon 561 (A561V), altering the fifth membrane-spanning domain (S5) of the HERG protein (Figure 4A). In K2596, an A to G substitution was identified at position 1408. This mutation results in substitution of aspartic acid for a conserved asparagine at codon 470 (N470D), located in the second membrane-spanning domain (S2) (Figure 4B). In K2015, a G to C substitution was identified. This substitution disrupts the splice-donor sequence of intron III, affecting the cyclic nucleotide-binding domain (Figure 4C). None of the aberrant conformers were identified in DNA samples from more than 200 unaffected individuals (data not shown).

De Novo Mutation of *HERG* in a Sporadic Case of LQT

To substantiate that *HERG* mutations cause LQT, we used SSCP analysis to screen for mutations in sporadic cases. Primer pair *4-12* identified an aberrant conformer in affected individual II-1 of K2269 (Figure 5). This conformer was not identified in either parent or in more than 200 unaffected individuals. Direct DNA sequencing of the aberrant conformer identified a G to A substitution at position 1882. This mutation results in substitution of serine for a highly conserved glycine at codon 628 (G628S), altering the pore-forming domain. Genotype analysis of this kindred using nine informative short tandem repeat polymorphisms confirmed maternity and paternity. The identification of a de novo mutation in a sporadic case demonstrates that *HERG* is *LQT2*.

HERG Is Expressed in the Heart

HERG was originally identified from a hippocampal cDNA library (Warmke and Ganetzky, 1994). To determine the tissue distribution of *HERG* mRNA, we isolated partial cDNA clones and used them in Northern blot analyses. Northern blot analyses showed strongest hybridization to heart mRNAs, with faint signals in brain, liver, and pancreas (Figure 6). Nonspecific hybridization was also seen in lung, possibly due to genomic DNA contamination. The size of the bands observed in cardiac mRNA was consis-

DOCKET ALARM

Explore Litigation Insights

Docket Alarm provides insights to develop a more informed litigation strategy and the peace of mind of knowing you're on top of things.

Real-Time Litigation Alerts

Keep your litigation team up-to-date with **real-time alerts** and advanced team management tools built for the enterprise, all while greatly reducing PACER spend.

Our comprehensive service means we can handle Federal, State, and Administrative courts across the country.

Advanced Docket Research

With over 230 million records, Docket Alarm's cloud-native docket research platform finds what other services can't. Coverage includes Federal, State, plus PTAB, TTAB, ITC and NLRB decisions, all in one place.

Identify arguments that have been successful in the past with full text, pinpoint searching. Link to case law cited within any court document via Fastcase.

Analytics At Your Fingertips

Learn what happened the last time a particular judge, opposing counsel or company faced cases similar to yours.

Advanced out-of-the-box PTAB and TTAB analytics are always at your fingertips.

API

Docket Alarm offers a powerful API (application programming interface) to developers that want to integrate case filings into their apps.

LAW FIRMS
Build custom dashboards for your attorneys and clients with live data direct from the court.

Automate many repetitive legal tasks like conflict checks, document management, and marketing.

FINANCIAL INSTITUTIONS
Litigation and bankruptcy checks for companies and debtors.

E-DISCOVERY AND LEGAL VENDORS
Sync your system to PACER to automate legal marketing.